Chinese Chemical Letters 34 (2023) 108329

Contents lists available at ScienceDirect

Chinese Chemical Letters

journal homepage: www.elsevier.com/locate/cclet

In vivo precision imaging of vicinal-dithiol-containing proteins by a FRET molecular probe sensitive to protein environment

Haocheng Gong[1], Yanhui Zhang[1], Ying Gao, Xinrong Tian, Pengzhao Wu, Xiaoyu Wei, Yuan Guo*

Key Laboratory of Synthetic and Natural Functional Molecule of the Ministry of Education, College of Chemistry and Materials Science, Northwest University, Xi'an 710127, China

ARTICLE INFO

Article history:
Received 11 December 2022
Revised 9 March 2023
Accepted 10 March 2023
Available online 13 March 2023

Keywords:
Vicinal-dithiol-containing proteins
Environment sensitivity
Super-resolution imaging
Fluorescent probes
Förster resonance energy transfer

ABSTRACT

We here present a Förster resonance energy transfer (FRET)-based and environment-sensitive fluorescent probe **VG-1** for vicinal-dithiol-containing proteins (VDPs). **VG-1** uniquely contains two sites sensitive to the protein environment (SPE), thus it shows weak fluorescence in both blue and green channels (a low FRET efficiency) in solution. After specifically binding with VDPs, its fluorescence in the green channel increases, while that in the blue channel disappears, achieving the specific detection of VDPs. The obvious signal changes in fluorescence may be attributed to that the increased rigidity of the molecular skeletons causes the enhanced FRET efficiency. The probe also achieved the cell super-resolution imaging of VDPs and the confocal imaging of VDPs in zebrafish.

Vicinal-dithiol-containing proteins (VDPs) are a class of proteins which contain at least one pair of thiol groups close in space at the reduced state [1,2]. The vicinal thiols in pairs exists in two forms including the HS-CXnC-SH, the main form composed of the juxtaposition of cysteinyl residues presented in distant segments of the same or different peptide chains, and HS-CC-SH, the rare form formed by cysteines proximal in sequence [2]. Normally, both forms contribute to the redox regulation within cells [3]. However, the overexpression of VDPs exacerbates cellular dysfunction and thus leads to an increased risk of diseases including cancer [4], Alzheimer's disease [5] and stroke [6], as this type of protein tends to react with reactive oxygen species under oxidative stress to form excessive disulfide-bonded proteins, a peroxide product. Thus, it is extremely necessary to develop tools for precisely detecting and tracking VDPs in biological systems.

In the recent years, various analytical approaches to detect VDPs have been developed, among which the fluorescence method has drawn much attention due to its excellent sensitivity, high temporal-spatial resolution and non-destructiveness [7–10]. As a result, plenty of VDPs fluorescent probes have been reported, some of which have achieved the imaging of VDPs *in vivo* [11,12]. Nevertheless, the fluorescent molecular probes available for selection in biological imaging of VDPs are still limited, and the molecular tools for the super-resolution imaging of VDPs in living cells are even scarcer. Thus, it is urgent to develop a powerful VDPs fluorescent probe which not only has excellent detection performance, but also can be used for the *in-vivo* precision imaging.

Various signaling mechanisms have been applied to the construction of VDPs fluorescent probes [11]. Among them, Förster resonance energy transfer (FRET) attracted extensive attention because the FRET-based probes showed excellent performance including low background interference and high sensitivity [13–16]. Normally, the switch of FRET process can be controlled through the modulation of the donor-acceptor spacing or the spectrum overlapping degree of donor emission and acceptor absorption [17–19]. While, the FRET efficiency of some environment-sensitive FRET probes largely depends on the specific environment that these molecules are in. This inspired us to design a FRET-based and environment-sensitive fluorescent probe **VG-1** for VDPs in this paper (Scheme 1). The probe uniquely contains two sites sensitive to the protein environment (SPE), thus it shows weak fluorescence in both blue and green channels (a low FRET efficiency) in solution. After specifically binding with VDPs, its fluorescence in the green channel increases, while that in the blue channel disappears, achieving the specific detection of VDPs. The obvious signal changes in fluorescence attributes to the increased rigidity of molecular skeleton which leads to the improvement of FRET efficiency. As such, **VG-1** is endowed with excellent

* Corresponding author.
E-mail address: guoyuan@nwu.edu.cn (Y. Guo).
[1] These authors contributed equally to this work.

https://doi.org/10.1016/j.cclet.2023.108329
1001-8417/

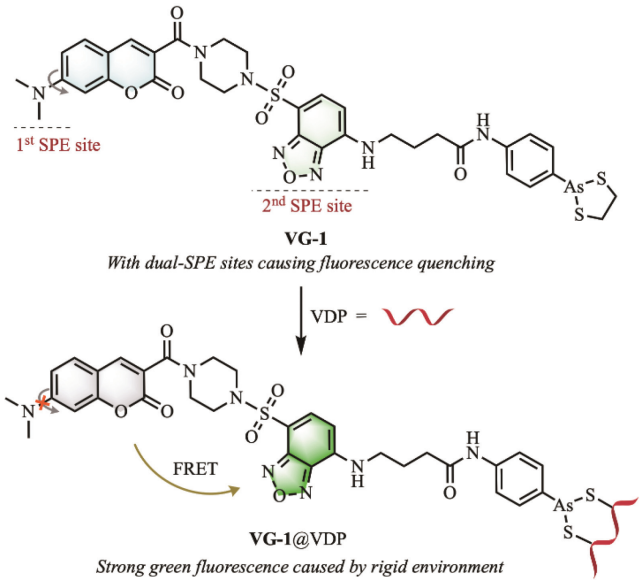

Scheme 1. Chemical structure of probe **VG-1** with dual-sites sensitive to the protein environment (SPE) and the proposed sensing mechanism of probe to VDPs.

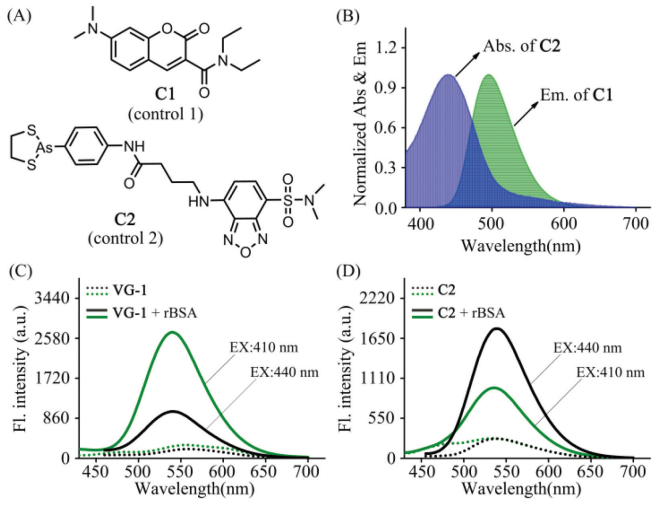

Fig. 1. (A) Chemical structures of control compounds **C1** and **C2** as the fluorescent analogues of FRET donor and FRET acceptor in **VG-1**, respectively. (B) Normalized absorption spectra of **C2** (2.0 μmol/L) and normalized emission spectra of **C1** (2.0 μmol/L) in Tris–HCl buffer solution (Tris–HCl:DMSO = 99.8:0.2, v/v, pH 7.4, 50 mmol/L, EX: 410 nm). (C, D) Fluorescence spectra of **VG-1** (C) and **C2** (D) with (solid line) and without (dotted line) rBSA (4.0 μmol/L) in Tris–HCl buffer solution (Tris–HCl:DMSO = 99.8:0.2, v/v, pH 7.4, 50 mmol/L). The green line shows the fluorescence spectra (C, D) with an excitation wavelength of 410 nm and the black line shows the fluorescence spectra (C, D) with an excitation wavelength of 440 nm. Slit = 5 nm/5 nm. Fl., fluorescence.

optical properties and biocompatibility, achieving the cell super-resolution imaging of VDPs and the confocal imaging of VDPs in zebrafish.

In detail, the fluorescent structure platform adopted by **VG-1** include two environment-sensitive fluorophores. One is a coumarin moiety mounted with a rotatable dimethylamino group and the other one is a 4-amino-7-aminosulfonylbenzo[*c*][1,2,5]oxadiazole (**ASBD**)-based skeleton with a large dipole moment. The former can act as the FRET donor for its outstanding emission efficiency, while the latter becomes the FRET acceptor for its absorption spectrum partly overlapping with emission spectrum of the donner. Due to the specific recognition of arsenic(III) to vicinal dithiols on VDPs [12,16], the cyclic dithiaarsane group installed in this platform can serve as the reaction site of VDPs. To verify the rationality of FRET process between the donor and the acceptor in **VG-1**, control compounds including **C1** derived from coumarin and benzoxadiazole-based **C2** were prepared. The structures of **C1** and **C2** are shown in Fig. 1A. The synthetic routes of probe **VG-1** and control compounds were depicted in Scheme S1 (Supporting information). The spectroscopic properties of control compounds **C1** and **C2** were then investigated, respectively. As shown in Fig. 1B**,** the fluorescence spectrum of **C1** clearly overlaps with the absorption spectrum of **C2**, which supports the FRET mechanism of **VG-1** constructed by the hybridization of the two related fluorophores. We also explored the environment sensitivity of probe **VG-1**. As shown in Fig. S1 (Supporting information), the fluorescence intensities of **VG-1** gradually increase with decreasing polarity or increasing viscosity, indicating that **VG-1** is highly sensitive to changes of environmental polarity and viscosity as expected.

With the above desired data in hands, the fluorescent sensing behavior of **VG-1** towards VDPs was then investigated. Reduced bovine serum albumin (rBSA) can serve as the *in-vitro* model protein of VDPs, because the reduced BSA has eight pairs of cysteines which are close in space [16]. As shown in Fig. 2A, the probe **VG-1** in aqueous solution showed negligible fluorescence in both blue and green channels due to the presence of dual-SPE sites capable of freely moving. After addition of rBSA, the green fluorescence elevated progressively with increasing concentrations of rBSA, and the fluorescence intensity of **VG-1** at 540 nm displayed a well linear relationship with the concentration of rBSA between 0 and 4.0 μmol/L. The limit of detection of VDPs was 78 nmol/L (Fig. 2A). These results proved the ability of probe **VG-1** to quantitatively determine VDPs. Besides, the fluorescence quantum yields (Φ) and molar extinction coefficients (ε) of **VG-1** before and after reaction with rBSA were calculated and summarized in Table S1 (Supporting information). In addition, the fluorescence response of **VG-1** to rBSA was further investigated using the same excitation wavelength (440 nm) as that of **ASBD**. As can be seen from Fig. 1C, the fluorescence intensity showed a 3.9-fold enhancement upon addition of rBSA, which is far less than that using the excitation wavelength of 410 nm (10.5-fold). Subsequently, the fluorescence response of the control compound **C2** toward rBSA was also evaluated (Fig. 1D). The fluorescence intensity at 540 nm showed a 3.5-fold increasement upon addition of rBSA with an excitation wavelength of 410 nm, while it exhibited a 6.6-fold enhancement with an excitation wavelength of 440 nm. Such results support the FRET effect from coumarin moiety to **ASBD**-based skeleton in **VG-1**. Moreover, it is worth noting that a distinct reduction in fluorescence intensity was observed after adding 1,2-ethanedithiol (EDT, a known specific ligand of trivalent arsenicals [20]) into the solution of the rBSA-**VG-1** complex (Fig. 2B), evidencing the availability of the cyclic dithiaarsane group as the VDPs reaction site. Meanwhile, the fluorescence intensity was decreased distinctly when guanidine hydrochloride (GndHCl, a strong protein denaturant [21]) was added into the solution of rBSA-**VG-1** complex (Fig. S2A in Supporting information), indicating that our probe **VG-1** is extremely sensitive to protein environment. Collectively, the fluorescence enhancement of the detection system was attributed to the location of the environmentally sensitive probe in a space-constrained environment upon the specifical binding of probe with rBSA.

Subsequently, the pH-dependent and time-dependent response of **VG-1** to VDPs were further investigated. As shown in Fig. 2C, the fluorescence intensity of **VG-1** was stable at pH values ranging from 3 to 9. Better still, **VG-1** showed satisfactory response to VDPs in the pH range of 6–9. The results demonstrate that probe **VG-1** can serve well as an excellent VDPs probe in physiological

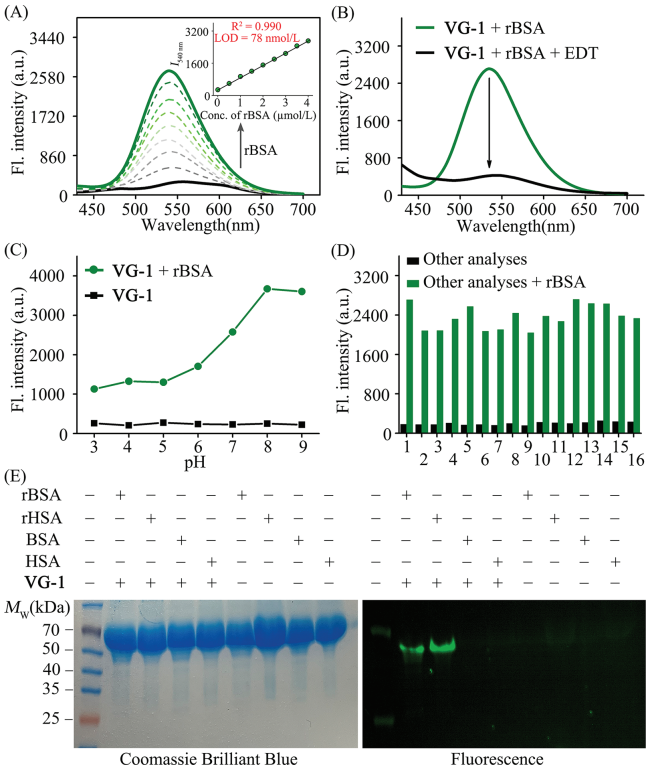

Fig. 2. (A) Fluorescence spectra of probe **VG-1** (2.0 μmol/L) in Tris–HCl buffer solution (Tris–HCl:DMSO = 99.8:0.2, v/v, pH 7.4, 50 mmol/L) upon addition of different concentrations of rBSA (0–4.0 μmol/L). (B) Fluorescence spectra of probe **VG-1** (2.0 μmol/L) with the addition of rBSA (4.0 μmol/L) in the presence (black) and absence (green) of EDT (1.0 mol/L) in Tris–HCl buffer solution (Tris–HCl:DMSO = 99.8:0.2, v/v, pH 7.4, 50 mmol/L). (C) Fluorescent intensity at 540 nm of **VG-1** (2.0 μmol/L) with (black) and without (green) rBSA (4.0 μmol/L) at various pH values in Tris–HCl buffer solution (50 mmol/L). (D) Selectivity and competition response of probe **VG-1** (2.0 μmol/L) to rBSA (4.0 μmol/L) against various amino acids (20 μmol/L), reductants (20 μmol/L) and proteins (4.0 μmol/L) at Tris–HCl buffer solution (Tris–HCl:DMSO = 99.8:0.2, v/v, pH 7.4, 50 mmol/L). 1. Blank, 2. Cys, 3. GSH, 4. Gly, 5. Lys, 6. Pro, 7. Val, 8. Ser, 9. Thr, 10. Arg, 11. Ascorbic acid, 12. TCEP, 13. DTT, 14. HSA, 15. *A. oryzae* β-gal, 16. BSA. (E) SDS-PAGE of VDPs and non-VDPs after treated or not treated with **VG-1**. "+": the compound was existent in the testing system; "−": the compound was inexistent in the testing system. EX: 410 nm, slit = 5 nm/5 nm.

environment. We then investigated the reaction kinetics of **VG-1** to VDPs. The fluorescence intensity of **VG-1** at 540 nm was negligible and almost had no significant changes within 12.0 h. While, upon adding rBSA (4.0 μmol/L) into the solution of probe **VG-1**, the fluorescence enhanced drastically and reached its maximum value in 6.0 h (Fig. S2B in Supporting information). Therefore, in order to obtain a precise and reproducible result, 6.0 h is adopted as an appropriate reaction time for VDPs assay.

Next, to test the selectivity of probe **VG-1** to VDPs, the fluorescent responses to some biologically relevant species were measured. As shown in Fig. 2D, only VDPs influenced the emission of probe **VG-1**, as expected. While, almost no distinct changes in fluorescence were appeared when **VG-1** was mixed with other interfering substance. Meanwhile, the specificity of **VG-1** toward VDPs was further confirmed by sodium dodecyl sulfate polyacrylamide gel electrophoresis (SDS-PAGE) (Fig. 2E). There was no obvious fluorescent band in the lane loaded with VDPs or non-VDPs. While, the lane loaded with both **VG-1** and VDPs displayed a remarkable fluorescence signal, and almost no fluorescence signal was observed in the lane loaded with both **VG-1** and non-VDP. Coomassie Brilliant Blue staining results proved that the fluorescent band was related to the formation of the VDPs-**VG-1** complex. These results indicated that the probe **VG-1** could achieve the highly selective detection of VDPs. To verify practical applicability of the probe, a competition experiment of **VG-1** in response to VDPs in the presence of other analytes was performed. After adding the rBSA into the mixture solution of **VG-1** and other competitive species, the evident fluorescence changes were still observed (Fig. 2D), suggesting that **VG-1** possesses good anti-interference capability for the detection of VDPs.

Next, we further explored the bio-imaging applications of **VG-1** in living HepG2 and A549 cells. Before imaging, the cytotoxicity of probe **VG-1** was investigated by using a standard MTT assay. The results showed that the toxicity of **VG-1** towards these cells was negligible even at a concentration up to 20 μmol/L (Fig. S3 in Supporting information). Subsequently, we test the potential capability of **VG-1** for detecting VDPs in living cells (Fig. 3A and B). Dithiothreitol (DTT) was used as a positive reagent to elevate the level of endogenous VDPs [22]. It can be seen that a weak fluorescence signal in the green channel could be observed when these DTT-untreated cells were incubated with **VG-1** for 20 min. While an obvious enhancement in the green channel was observed when the cells were pre-stimulated with DTT and further treated with **VG-1** for 20 min, which supports the specificity of **VG-1** to VDPs in living cells and an appropriate incubation time of 20 min. It's worth noting that the fluorescence changes were absolutely reversed when the cells were pretreated with 4-aminophenylarsenoxide (PAO), a known specific ligand of VDPs [23], further confirming its targeting towards VDPs. These above results suggest that our probe **VG-1** is satisfying and reliable whether in biocompatibility or in selectivity and can be used for the detection of VDPs in living cells. Subsequently, the distribution of VDPs was investigated by super-resolution imaging. As displayed in Fig. 3C, the features of mitochondria were clearly observed in DTT-treated A549 cells by the super-resolution imaging. Meanwhile, the fluorescence of probe **VG-1** in the green channel overlapped well with that of MitoTracker in the red channel. The cell SIM images provided high-resolution visualization of VDPs mainly distributed in mitochondria. We here wish to clarify that our probe **VG-1** has the definite ability to detect VDPs in the whole cell and does not target mitochondria. The reason why VDPs were mainly found in mitochondria in our SIM images is that VDPs themselves are mainly distributed in mitochondria [12,16,23].

Encouraged by the above results, we sought to test the ability of **VG-1** *in vivo* by imaging VDPs in 5-day-old zebrafish. As shown in Fig. 3D, after incubation with **VG-1**, zebrafish exhibited a weak green fluorescence signal. When zebrafish were pre-treated with DTT and further incubated with **VG-1**, a remarkable enhancement of green fluorescence was observed. These results clearly displayed that probe **VG-1** owns the ability to detect VDPs in zebrafish, demonstrating its significant potential to investigate VDPs-associated pathological processes through *in-vivo* imaging.

To summarize, we have developed a FRET-based fluorescent probe **VG-1** for VDPs by using 1,3,2-dithiarsolan as the recognition site, coumarin moiety as the FRET donor, and **ASBD**-based skeleton as the FRET acceptor. Uniquely, the probe showed a low FRET efficiency in solutions due to both donor and acceptor fluorophores highly sensitive to environment, resulting in weak fluorescence in both blue and green channels. After specifically binding with VDPs, the fluorescence of the probe located in the space-limited environment was increased in the green channel while disappeared in the blue channel, achieving the FRET-based detection of VDPs. **VG-1** displayed excellent sensitivity, high signal-to-noise ratio, and good specificity toward VDPs over various biothiols and other proteins. Importantly, the probe with low background interference has successfully achieved the cell super-resolution imaging of VDPs and the confocal imaging of VDPs in zebrafish.

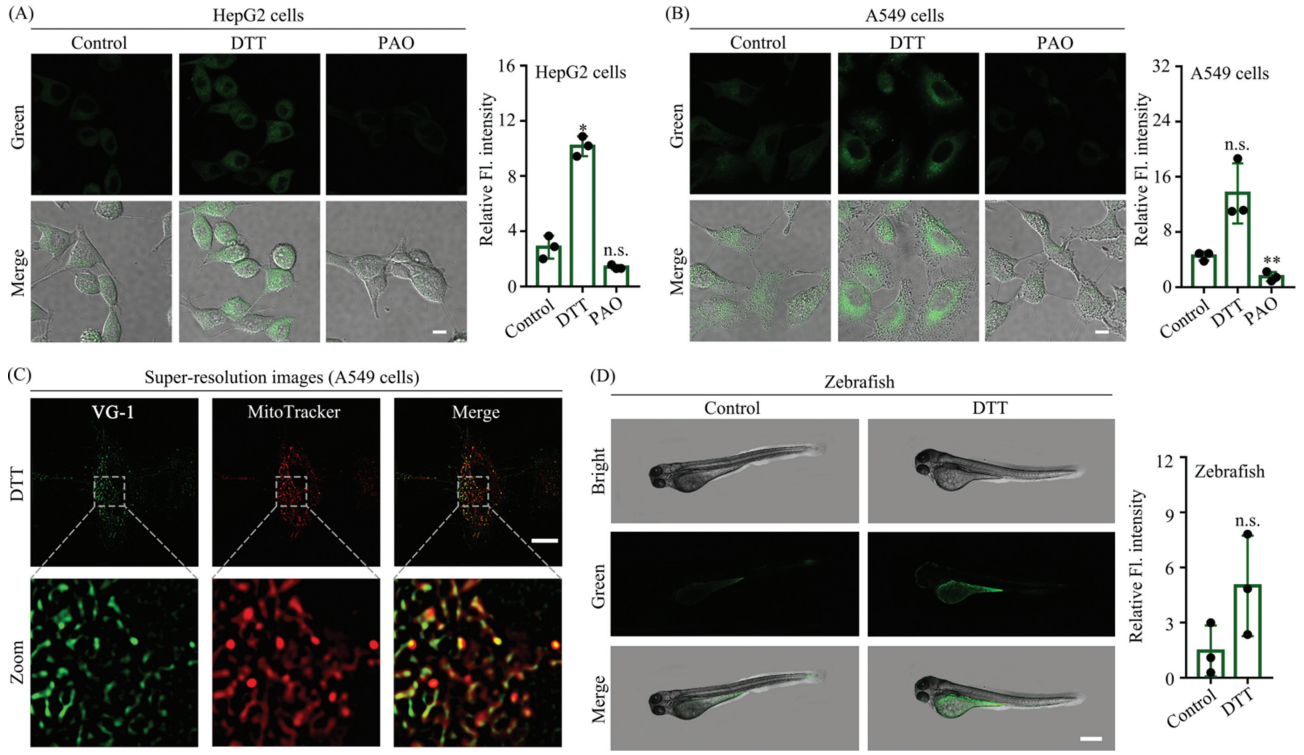

Fig. 3. (A, B) Confocal imaging of VDPs in HepG2 cells (A) and A549 cells (B) by using **VG-1**, respectively. Column 1: cells were treated with **VG-1**. Column 2: cells were pretreated with DTT, subsequently incubated with **VG-1**. Column 3: cells were pretreated with PAO, subsequently incubated with **VG-1**. Column 4: average fluorescent intensity of **VG-1**-stained HepG2 cells (A) and A549 cells (B). Scale bar = 20 μm. (C) Super-resolution images of VDPs in DTT-treated A549 cells stained by **VG-1** and the zoomed image. A549 cells were pre-stimulated with DTT, then incubated with **VG-1**, followed incubated with MitoTracker Deep Red. Scale bar = 10 μm. (D) Imaging VDPs in zebrafishes (left) and the average fluorescence intensity (right) from parallel images including (D, left). Column 1: zebrafishes were incubated with **VG-1**. Column 2: zebrafishes were incubated with DTT, subsequently incubated with **VG-1**. Scale bar = 500 μm. Data were expressed as mean ± standard deviation (S.D.), $n = 3$. The number of dots represents the number of samples. The significant differences (n.s., not significant. $^{*}P < 0.05$, $^{**}P < 0.01$ *vs.* control were analyzed with two-sided Student's *t*-test.

Declaration of competing interest

The authors declare that they have no known competing financial interests or personal relationships that could have appeared to influence the work reported in this paper.

Acknowledgments

We thank the National Natural Science Foundation of China (Nos. 21977082, 22037002 and 21472148) and the Natural Science Basic Research Program of Shaanxi (No. 2020JC-38).

Supplementary materials

Supplementary material associated with this article can be found, in the online version, at doi:10.1016/j.cclet.2023.108329.

References

[1] C. Gitler, M. Mogyoros, E. Kalef, Methods Enzymol. 233 (1994) 403–415.
[2] D.M. Ziegler, Ann. Rev. Biochem. 54 (1985) 305–329.
[3] J. Ying, N. Clavreul, M. Sethuraman, T. Adachi, R.A. Cohen, Free Radic. Biol. Med. 43 (2007) 1099–1108.
[4] X.W. Zhang, X.J. Yan, Z.R. Zhou, et al., Science 328 (2010) 240–243.
[5] C. Zhang, C. Rodriguez, J. Spaulding, T.Y. Aw, J. Feng, J. Alzheimers Dis. 28 (2012) 655–666.
[6] M.L. Alexandrova, P.G. Bochev, Free Radic. Biol. Med. 39 (2005) 297–316.
[7] Y. Yue, T. Zhao, Y. Wang, et al., Chem. Sci. 13 (2022) 218–224.
[8] Y. Yang, T. Zhou, M. Jin, et al., J. Am. Chem. Soc. 1422 (2020) 1614–1620.
[9] D. Ma, S. Hou, C. Bae, et al., Chin. Chem. Lett. 32 (2021) 3886–3889.
[10] D. Shi, W. Liu, G. Wang, Y. Guo, J. Li, Acta Mater. Med. 1 (2022) 4–23.
[11] X. Wei, T. Jin, C. Huang, et al., Chem. Rev. 429 (2021) 213621.
[12] G. Hu, H. Jia, L. Zhao, et al., Chin. Chem. Lett. 30 (2019) 1704–1716.
[13] M. Li, F. Wang, L. Yan, et al., Chem. Commun. 58 (2022) 10186.
[14] B. Prevo, E.J.G. Peterman, Chem. Soc. Rev. 43 (2014) 1144–1155.
[15] J. Fan, M. Hu, P. Zhan, X. Peng, Chem. Soc. Rev. 42 (2013) 29–43.
[16] C. Huang, T. Jia, M. Tang, et al., J. Am. Chem. Soc. 136 (2014) 14237–14244.
[17] L. He, W. Lin, Q. Xu, H. Wei, Chem. Commun. 51 (2015) 1510–1513.
[18] T. Li, F. Huo, J. Chao, C. Yin, Chem. Commun. 56 (2020) 11453–11456.
[19] J. Wang, J. Li, Z. Yu, et al., Anal. Chem. 94 (2022) 14029–14037.
[20] W.L. Zahler, W.W. Cleland, J. Biol. Chem. 243 (1968) 716–719.
[21] Y. Hong, C. Feng, Y. Yu, et al., Anal. Chem. 82 (2010) 7035–7043.
[22] Y. He, J. Shin, W. Gong, et al., Chem. Commun. 55 (2019) 2453–2456.
[23] F. Liu, H.J. Liu, X.J. Liu, et al., Anal. Chem. 89 (2017) 11203–11207.